The dependence of the phase diagram on the range of the attractive intermolecular forces

1997 J. Phys.: Condens. Matter 9 3361

(http://iopscience.iop.org/0953-8984/9/16/008)

J. Phys.: Condens. Matter **9** (1997) 3361–3370. Printed in the UK PII: S0953-8984(97)77116-9

The dependence of the phase diagram on the range of the attractive intermolecular forces

M Hasegawa† and K Ohno‡

† Department of Materials Science and Technology, Faculty of Engineering, Iwate University, Morioka 020, Japan

‡ Institute for Materials Research, Tohoku University, Sendai 980-77, Japan

Received 12 August 1996

Abstract. A density functional theory of freezing combined with a thermodynamically consistent integral equation method is used to investigate the phase behaviour of systems interacting via the m–n potential with $m = 2n$, $\phi(r) = 4\varepsilon[(\sigma/r)^{2n} - (\sigma/r)^n]$ ($n = 6$, 8, 10 and 12) and rigid C_{60} molecules interacting via the Girifalco potential. It is found that the liquid–vapour coexistence region is gradually suppressed as the attractive part of the potential becomes short range with increasing n and the coexistence ceases to occur at $n \approx 11$. The m–n potential with $n = 11$–12 is similar to the Girifalco potential and the two yield similar phase diagrams. It is also found that the phase diagram of C_{60} calculated for a truncated potential is qualitatively in agreement with the corresponding Monte Carlo (MC) simulations of Hagen *et al*, which have predicted nonexistence of the liquid phase in contrast to the molecular dynamics (MD) simulations of Cheng *et al*. These results suggest the importance of treating the long-range tail of the potential correctly and provide a partial explanation for the discrepancy between the MC and MD simulations.

1. Introduction

For ordinary atomic or molecular systems interacting via potentials with sufficiently strong attractive forces, liquid–vapour coexistence occurs and the liquid exists as a stable phase. However, if the range or intensity of the attractive part of the intermolecular potential becomes sufficiently small, the sublimation line passes above the liquid–vapour critical point and the liquid phase no longer exists. This observation has been made in the theoretical investigation for the colloidal suspension [1]. Recently, the phase behaviour of simple systems with short-range or weak attractive intermolecular forces has also attracted increasing attention. One such example that has emerged in recent years is the phase behaviour of C_{60} molecules [2], and several simulation and theoretical studies have been performed to determine their phase diagram using the intermolecular potential proposed by Girifalco [3]. Hagen *et al* have performed Monte Carlo (MC) simulations and concluded that C_{60} has no liquid phase [4], whereas the molecular dynamics (MD) simulations of Cheng *et al* have predicted that the liquid phase exists in a narrow range of temperatures [5]. Mederos and Navascués have discussed these contradictory results using their density functional theory (DFT) of freezing but concluded that the theory cannot definitively settle this point [6]. On the other hand, Caccamo has used the modified hypernetted-chain (MHNC) theory together with the empirical one-phase criterion for the freezing and obtained a result which is in agreement with the MD simulations [7]. We have also performed similar

0953-8984/97/163361+10$19.50

calculations using our DFT of freezing in place of the empirical criterion [8]. Our result is in qualitative agreement with the MD simulations and Caccomo's results but the predicted range of the liquid phase is much narrower (< 20 K). These results suggest that C_{60} is a critical substance which might have a liquid phase or not, but its phase behaviour is still not very conclusive.

The effect of short-rangedness or weakness of the attractive intermolecular forces on the phase behaviour has also been investigated for some model systems by simulations [9–12], the DFT of freezing, and other theories such as the van der Waals theory [13–17]. These studies have shown that the liquid–vapour coexistence ceases to occur if the attractive force is reduced to a critical strength depending on the nature of individual potential. The effect of the short-rangedness of the intermolecular potential on the isostructural solid-to-solid transition has also been the issue of considerable interest and several theoretical investigations have been made [18–23].

In this paper we present a DFT for the phase behaviour of systems with varying range of attractive forces. We first consider systems interacting via the *m–n* potentials. This part of the present work may constitute a theoretical complement of the MC simulation studies of Hafskjold [11], who has considered systems interacting via the *m–n*–spline potential, which is a 'truncated' version of the *m–n* potential. C_{60} is also revisited and the effect on the phase diagram of truncating the long-range tail of the potential is examined. In simulation studies such a truncation has often been made for practical reasons but could lead to a quite different result as actually confirmed for the Lennard-Jones (LJ) fluid [9]. In this work we use a generalized version of the modified weighted-density approximation (MWDA) combined with a thermodynamically consistent integral equation method. The generalized MWDA (GMWDA) is a generalization of the MWDA of Denton and Ashcroft [24], and has been successfully applied to inverse-power systems [25]. The preliminary report of the present study on C_{60} is found elsewhere [8].

In the next section we summarize the GMWDA. In section 3 the prescriptions are given for applications to *m–n* potential systems and C_{60}, and the results of calculations are presented. The final section is devoted to the summary and conclusions.

2. Summary of the GMWDA

We consider a non-Coulombic system interacting through a pair potential, $\phi(r)$, which decays more rapidly than r^{-3} as $r \to \infty$. Following the thermodynamic perturbation theory developed for uniform liquids [26], we start by splitting $\phi(r)$ into two parts, $\phi(r) = \phi_0(r) + \Delta\phi(r)$, where $\phi_0(r)$ is a repulsive, short-range part and $\Delta\phi(r)$ is the remaining long-range part. The (Helmholtz) free energy of the system as a functional of the (number) density $\rho(\boldsymbol{r})$ is then written, in accordance with the above potential splitting, as

$$F[\rho] = F_{id}[\rho] + F_{0,ex}[\rho] + F_1[\rho] \tag{1}$$

where $F_{id}[\rho]$ is the ideal-gas contribution, $F_{0,ex}[\rho]$ the excess free energy of the *reference* system interacting through $\phi_0(r)$, and $F_1[\rho]$ the contribution due to $\Delta\phi(r)$. The functional form of $F_{id}[\rho]$ is given by

$$F_{id}[\rho] = \beta^{-1} \int \mathrm{d}\boldsymbol{r}\, \rho(\boldsymbol{r})\{\ln[\rho(\boldsymbol{r})\Lambda^3] - 1\} \tag{2}$$

where β is the inverse temperature, $\beta = 1/k_B T$, and Λ is the thermal de Broglie wavelength. The contribution $F_1[\rho]$ is formally written as [26]

$$F_1[\rho] = \frac{1}{2}\int \mathrm{d}\boldsymbol{r}_1 \int \mathrm{d}\boldsymbol{r}_2 \int_0^1 \mathrm{d}\lambda\, \rho_\lambda^{(2)}(\boldsymbol{r}_1, \boldsymbol{r}_2)\Delta\phi(r_{12}) \tag{3}$$

where $\rho_\lambda^{(2)}$ is the pair distribution function of a system interacting through $\phi_\lambda(r) = \phi_0(r) + \lambda\Delta\phi(r)$ and $r_{12} = |\boldsymbol{r}_1 - \boldsymbol{r}_2|$.

For an appropriate potential separation the reference free energy $F_{0,ex}[\rho]$ is mostly entropic and the contribution $F_1[\rho]$ accounts for most of the cohesive energy. Curtin and Ashcroft noted the importance of treating these contributions by separate approximations [27]. Since then various versions based on the above approach have been developed and the major differences between them consist in the choice of the reference system and in the treatment of $F_1[\rho]$ [25, 27–30]. The hard-sphere (HS) system has most often been employed as the reference system and treated by nonperturbative DFT such as the weighted-density approximation (WDA) [31], the modified WDA (MWDA) [24], and the generalized effective-liquid approximation (GELA) [32]. On the other hand, the contribution $F_1[\rho]$ has been calculated by introducing approximations to $\rho_\lambda^{(2)}$ in (3) [28–30], or by using the second-order perturbation theory [27],

$$F_1[\rho] \approx F_1(\bar{\rho}) - \frac{1}{2\beta}\int \mathrm{d}\boldsymbol{r}_1 \int \mathrm{d}\boldsymbol{r}_2\, \Delta C^{(2)}(\boldsymbol{r}_{12}; \bar{\rho})\Delta\rho(\boldsymbol{r}_1)\Delta\rho(\boldsymbol{r}_2). \tag{4}$$

In equation (4) $\Delta C^{(2)} = C^{(2)} - C_0^{(2)}$, where $C^{(2)}$ and $C_0^{(2)}$ are the two-particle direct correlation functions (DCFs) of the full and reference systems, respectively, and $\Delta\rho(\boldsymbol{r}) = \rho(\boldsymbol{r}) - \bar{\rho}$, $\bar{\rho}$ being the average density of the solid under consideration.

The GMWDA is quite similar to the theory of Curtin and Ashcroft [27], and it is based on the separate global thermodynamic mappings for $F_{0,ex}[\rho]$ and $F_1[\rho]$ [25]:

$$F_{0,ex}[\rho] \approx N f_{0,ex}(\hat{\rho}_0) \tag{5a}$$

and

$$F_1[\rho] \approx N f_1(\hat{\rho}_1) \tag{5b}$$

where N is the number of particles in the system, $f_{0,ex}(\rho)$ the excess free energy per particle of a uniform reference fluid and $f_1(\rho)$ the contribution due to $\Delta\phi(r)$, i.e. $f_1(\rho) = f_{ex}(\rho) - f_{0,ex}(\rho)$, $f_{ex}(\rho)$ being the total excess free energy per particle of the system. We assume that the effective-liquid densities, $\hat{\rho}_0$ and $\hat{\rho}_1$, are independent of each other and given by

$$\hat{\rho}_0 = \frac{1}{N}\int \mathrm{d}\boldsymbol{r}_1 \int \mathrm{d}\boldsymbol{r}_2\, \rho(\boldsymbol{r}_1)\rho(\boldsymbol{r}_2)w_0(r_{12}; \hat{\rho}_0) \tag{6a}$$

and

$$\hat{\rho}_1 = \frac{1}{N}\int \mathrm{d}\boldsymbol{r}_1 \int \mathrm{d}\boldsymbol{r}_2\, \rho(\boldsymbol{r}_1)\rho(\boldsymbol{r}_2)w_1(r_{12}; \hat{\rho}_1) \tag{6b}$$

as in the original MWDA [24]. The weight functions w_0 and w_1, as yet unspecified, are determined by two requirements. The first one is that both w_0 and w_1 are normalized, which must be satisfied in the limit of a uniform density to ensure that the approximation scheme becomes exact in this limit. The second requirement is that the approximate $F_{0,ex}[\rho]$ and $F_1[\rho]$ in (5*a*) and (5*b*) exactly reproduce the corresponding two-body DCFs, i.e. $C_0^{(2)}(r; \rho)$ and $\Delta C^{(2)}(r; \rho)$, respectively, in the limit of uniform density. Unique specifications of the

weight functions follow from these requirements and the substitution of these results into (6*a*) and (6*b*) leads to the implicit equations for $\hat{\rho}_0$ and $\hat{\rho}_1$ [25],

$$(\hat{\rho}_0 - \bar{\rho})\beta f'_{0,ex}(\hat{\rho}_0) = -\frac{1}{2N}\int \mathrm{d}\boldsymbol{r}_1 \int \mathrm{d}\boldsymbol{r}_2\, \Delta\rho(\boldsymbol{r}_1)\Delta\rho(\boldsymbol{r}_2)C_0^{(2)}(r_{12};\hat{\rho}_0) \qquad (7a)$$

and

$$(\hat{\rho}_1 - \bar{\rho})\beta f'_1(\hat{\rho}_1) = -\frac{1}{2N}\int \mathrm{d}\boldsymbol{r}_1 \int \mathrm{d}\boldsymbol{r}_2\, \Delta\rho(\boldsymbol{r}_1)\Delta\rho(\boldsymbol{r}_2)\Delta C^{(2)}(r_{12};\hat{\rho}_1) \qquad (7b)$$

where $f'_{0,ex}(\rho) = \partial f_{0,ex}(\rho)/\partial\rho$ and $f'_1(\rho) = \partial f_1(\rho)/\partial\rho$. We note that both $\hat{\rho}_0$ and $\hat{\rho}_1$ are functionals of $\rho(\boldsymbol{r})$ and determined by solving (7*a*) and (7*b*), respectively, for a given $\rho(\boldsymbol{r})$. The approximate excess free energy per particle is then given by

$$\beta f_{ex}[\rho] = \beta f_{0,ex}(\hat{\rho}_0) + \beta f_1(\hat{\rho}_1). \qquad (8)$$

We also note that we must follow Laird and Kroll [33] to derive the GMWDA for the Coulombic systems such as the classical one-component plasma (OCP) [25].

In the GMWDA we have used the MWDA separately to calculate both $F_{0,ex}[\rho]$ and $F_1[\rho]$, but other theories also could have been used. In fact, the WDA and the GELA are useful candidates for calculating $F_{0,ex}[\rho]$ (the GELA works only for the HS reference system). However, we gain little by the use of these theories, while the implementation of these theories is much more demanding than that of the MWDA.

3. Applications to the *m–n* potential systems and C_{60}

3.1. Prescriptions

Following Hafskjold [11], we considered systems interacting through *m–n* potentials with $m = 2n$, i.e.

$$\phi(r) = 4\varepsilon[(\sigma/r)^{2n} - (\sigma/r)^n]. \qquad (9)$$

The LJ potential corresponds to the case of $n = 6$. The *m–n*–spline potential used by Hafskjold in the MC simulations is a 'truncated' version of (9), i.e. it is given by (9) for $r < r_s$, where r_s is the inflection point of $\phi(r)$, but modified as $\phi(r) = c(r-r_c)^2 + d(r-r_c)^3$ for $r_s < r < r_c$ and $\phi(r) = 0$ for $r > r_c$. Here the parameters c, d and r_c are determined by the requirement that the modified potential and its first- and second-order derivatives are continuous at $r = r_s$ [11, 34]. As the first step in our theoretical investigations we considered only the *m–n* potentials given by (9). Another system we considered is C_{60} molecules interacting via the potential proposed by Girifalco [3], which is given by

$$\phi(r) = -A[1/s(s-1)^3 + 1/s(s+1)^3 - 2/s^4] + B[1/s(s-1)^9 + 1/s(s+1)^9 - 2/s^{10}] \qquad (10)$$

where $s = r/2a$ and $2a = 0.71$ nm. This potential has been obtained by assuming that the carbon atoms on different C_{60} molecules interact through an LJ potential and that the carbon atoms on each C_{60} molecule are uniformly distributed on the spherical surface with diameter $2a$. This spherical approximation may be justified at high temperatures, where C_{60} molecules are almost freely rotating. The parameters A and B in (10) were determined empirically and are given in [3]. This potential is compared with the *m–n* potentials with $n = 6$, 8, 10 and 12 in figure 1. For the Girifalco potential $\sigma/2a = 1.351\,113$ and $r_0/2a = 1.141\,634$, where σ and r_0 are the distances at which $\phi(r)$ crosses zero and takes the principal minimum, respectively. We find that the *m–n* potential with $n = 11$–12 is

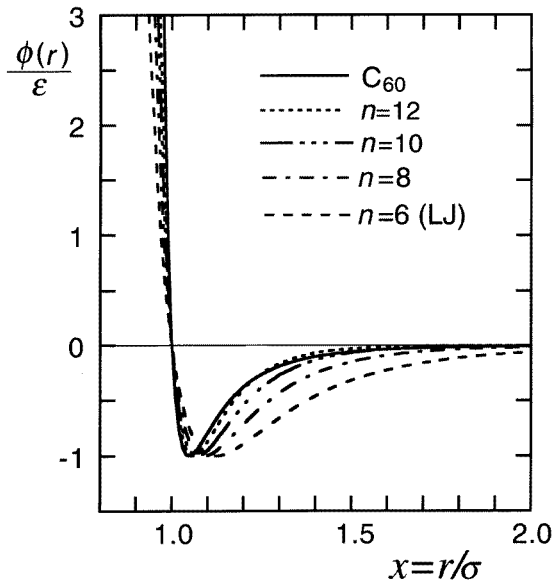

Figure 1. Comparisons of the m–n potentials and the Girifalco potential for C_{60}, for which $\sigma/2a = 1.351\,113$ and the well depth is 3218 K.

very similar to the Girifalco potential if they are scaled by the well depth and plotted as the functions of the scaled distance, r/σ.

In the MC simulations for C_{60} [4], the potential given by (10) was truncated at $r = 2\sigma$ ($s = 2.70$), where the magnitude of $\phi(r)$ is very small and only 0.76% of the well depth. We also used a 'truncated' potential which is smooth for convenience in solving the integral equation (see below) but mimics the one used in the MC simulations:

$$\phi_{trunc}(\boldsymbol{r}) = \begin{cases} \phi(r) & r < r_1 \\ \phi(r_1)\,\mathrm{e}^{-\lambda(r-r_1)} & r > r_1 \end{cases} \tag{11}$$

where $\phi(r)$ is given by (10) and $\lambda = -\phi'(r_1)/\phi(r_1)$, which ensures the continuity of $\phi'_{trunc}(r)$ at $r = r_1$. We used the value $s_1 = r_1/2a = 2.0$, which was determined by requiring that the potential (11) and the one used in the MC simulations [4] yield the same Fourier transform in the long-wavelength limit, i.e. approximately the same internal energy and virial pressure.

In the applications of the GMWDA to the systems characterized by equations (9)–(11) we employed the potential separation proposed by Weeks, Chandler and Andersen (WCA) [35], which is defined by

$$\phi_0(\boldsymbol{r}) = \begin{cases} \phi(r) - \phi(r_0) & r < r_0 \\ 0 & r > r_0 \end{cases} \tag{12}$$

where r_0 is, as before, the separation at which $\phi(r)$ takes the principal minimum. As noted above the HS system has been the most popular reference system in the thermodynamic perturbation approach. However, we did not use the HS system as the reference system in the present work because of the unfavourable features found in our previous work [36]. We first note that, if we use accurate input data in place of the approximate Percus–Yevick

(PY) ones in the MWDA and GELA equations for the HS system, the predicted freezing parameters slightly worsen. Furthermore, such a unfavourable feature becomes much more serious when the HS system is used as the reference system. In fact, as demonstrated for the OCP, reasonable freezing properties cannot be predicted unless we use the approximate PY DCF and the corresponding free energy rather than more accurate ones in the MWDA and GELA used to treat the reference HS system [36].

The modified hypernetted-chain (MHNC) theory [37] was used to calculate the equation of state and DCFs of the systems interacting through $\phi(r)$ and $\phi_0(r)$, which are the necessary input to solve equations (7*a*) and (7*b*) and to determine the liquid–vapour phase boundary. Among the several versions in the context of the MHNC theory we used the thermodynamically consistent one. More explicitly, we used the accurate HS bridge function derived from the Verlet–Weis parametrization of the HS radial distribution function [38, 39], and determined the HS parameter such that the virial pressure and compressibility equations are consistent with each other. The details of the method for solving the MHNC equations are given elsewhere [7, 8].

In the calculations of the free energy of the solid phase in the GMWDA we followed the common practice and used a variational method, in which the density distribution in the solid was parametrized as

$$\rho(\boldsymbol{r}) = \left(\frac{\alpha}{\pi}\right)^{3/2} \sum_{\boldsymbol{R}} \exp[-\alpha(\boldsymbol{r} - \boldsymbol{R})^2] \tag{13}$$

where $\{\boldsymbol{R}\}$ is the Bravais lattice vectors. We solved equations (7*a*) and (7*b*) for varying values of α and minimized the resulting free energy of the solid,

$$\beta f(\bar{\rho}; \alpha) = \beta f_{id}(\bar{\rho}; \alpha) + \beta f_{ex}(\bar{\rho}; \alpha) \tag{14}$$

with respect to α, where $\beta f_{ex}(\bar{\rho}; \alpha)$ is obtained from (8). The method of calculating the ideal-gas contribution $\beta f_{id}(\bar{\rho}; \alpha)$ has been given elsewhere [32]. In the actual calculations it is convenient to calculate the solid free energy relative to the liquid with the same density, i.e.

$$\beta \Delta f(\bar{\rho}) = \beta f_{solid}(\bar{\rho}) - \beta f_{liq}(\bar{\rho}) \tag{15}$$

where $\beta f_{solid}(\bar{\rho}) = \beta f(\bar{\rho}; \alpha)$ and $\beta f_{liq}(\bar{\rho}) = \beta f(\bar{\rho}; \alpha = 0)$.

3.2. Results

The liquid–vapour and the solid–liquid phase boundaries were determined by enforcing equality of pressures and chemical potentials in the two coexisting phases at a fixed temperature. Figure 2 illustrates the phase diagram of the LJ system obtained by the present theory and its comparisons with the MC simulations [40, 41]. The face-centred-cubic (fcc) structure is assumed for the solid phase in these studies. Hereafter we use the reduced temperature and density defined by $T^* = k_B T/\varepsilon$ and $\rho^* = \rho\sigma^3$, respectively, for the m–n potential systems. We find that the present result for the liquid–vapour phase boundary is in good agreement with the MC simulations [40], yielding the critical temperature $T_c^* \sim 1.32$. This part of the phase diagram is determined solely by the fluid data and is essentially the same as that of Caccamo [7]. The present and MC results for the melting line are also in good agreement with each other. However, the present result for the freezing line falls at somewhat lower densities and yields a higher triple point, $T_t^* \sim 0.80$, than the MC result, $T_t* \sim 0.70$. This discrepancy for the freezing line may be ascribed to the defect of the MWDA for the reference system as well as for the HS system (equation (7*a*)). In fact, the freezing density of the HS system predicted by the MWDA is about 3–5% smaller than the

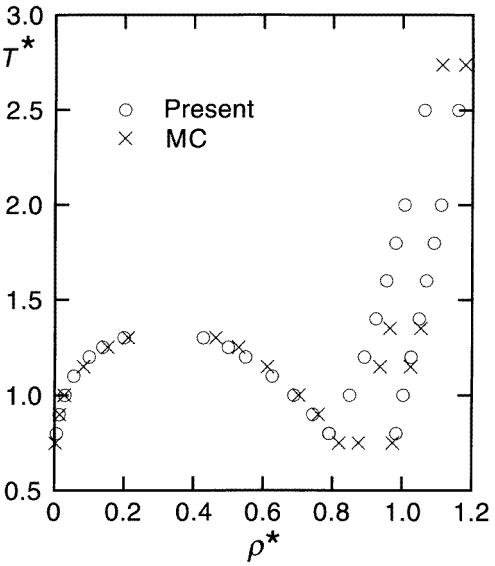

Figure 2. The predicted phase diagram of the LJ system and its comparisons with the MC results from [40] for the solid–liquid coexistence and from [41] for the liquid–vapour coexistence. The fcc structure is assumed for the solid phase, and T^* and ρ^* are defined by $T^* = k_B T/\varepsilon$ and $\rho^* = \rho\sigma^3$, respectively.

MC results, whereas the MWDA and MC have predicted much the same melting density [24, 33, 36].

The predicted phase behaviours of the *m–n* potential systems are summarized in figure 3. The fcc structure is also assumed for the solid phase in all these calculations. We find that the liquid–vapour coexistence region is suppressed as the potential becomes short range with increasing n and the coexistence ceases to occur for large n. These results are qualitatively similar to those found for other systems such as the one interacting through the hard-core–attractive Yukawa potential [10, 13]. The critical value of n separating existence and nonexistence of a liquid phase is between 10 and 12, i.e. $n_c \sim 11$, in the present GMWDA. However, as noted above the freezing line predicted by the GMWDA could fall at somewhat lower densities than the true result, yielding a higher triple point. If this feature of the GMWDA is taken into account, the true critical value could be larger, i.e. $n_c \sim 12$. We note that for large n (> 8) the effect of truncating $\phi(r)$ in (9) becomes less significant and the present results for the *m–n* potentials are similar to those for the corresponding *m–n*–spline potentials obtained by the MC simulations [11], which have predicted a smaller value, $n_c \sim 10$, reflecting the effect of truncation.

Figure 4 shows the phase diagrams of C_{60} predicted by the GMWDA using the full and truncated potentials. The freezing line obtained for the full potential crosses the liquid–vapour binodal line slightly below the estimated critical temperature, $T_c = 1960$ K, and the liquid phase does exist albeit in a very narrow range of temperatures (< 20 K) [8]. If we use a 'truncated' potential the liquid–vapour phase boundary is shifted downwards by ~ 100 K and the sublimation line now passes about 50 K above the critical point. This result is qualitatively in agreement with the MC simulations of Hagen *et al* [4], in which the truncated potential was used. As noted above the Girifalco potential (10) is quite small ($\sim 0.76\%$ of the well depth) at the truncation point, $r = 2\sigma$, but the effect of truncation

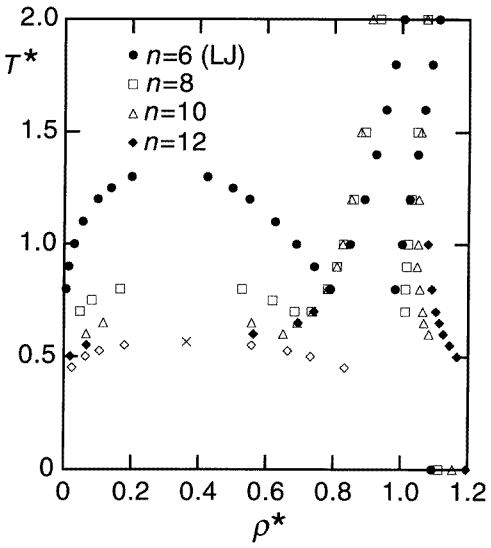

Figure 3. Predicted phase diagrams of the m–n potential systems. The fcc structure is also assumed for the solid phase, and T^* and ρ^* are the reduced quantities as in figure 2. Open diamonds (◇) show the boundary of the (metastable) liquid–vapour coexistence region for $n = 12$ and the cross (×) is the estimated critical point, which lies below the sublimation line (◆).

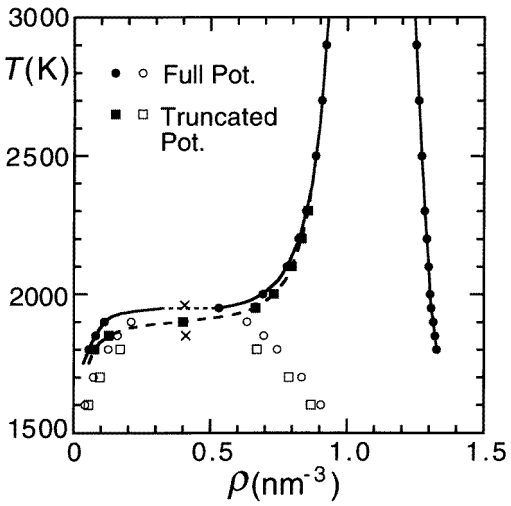

Figure 4. Phase diagrams of C_{60} predicted for the Girifalco potential (10) and for its 'truncated' version given by (11). Open circles and open squares represent the boundaries of the (metastable) liquid–vapour coexisting region and crosses show the estimated critical points. The melting line for the truncated potential is almost indistinguishable from that for the full potential.

on the equation of state is significant, amounting to a $\sim 5\%$ reduction in magnitude of the free energy of the fluids, which leads to a $\sim 5\%$ (~ 100 K) shift of the liquid–vapour phase boundary as actually seen in figure 4. These results suggest the importance of treating the long-range tail of the potential correctly even in the study of the phase diagram of C_{60}.

For the LJ system the effect of the potential truncation (at $r = 2.5\sigma$) on the liquid–vapour coexistence has been found to be much more significant [9]. We also note that the predicted phase diagram of C_{60} is quite similar to that of the m–n potential system with $n \sim 11$, which could have been anticipated from the similarity of the potentials as illustrated in figure 1.

4. Summary and conclusions

We have applied the GMWDA combined with a thermodynamically consistent integral equation method to the calculations of the phase diagram of m–n potential systems and C_{60} molecules interacting via the Girifalco potential. We have confirmed that the liquid–vapour coexistence region of the m–n potential systems is suppressed as the attractive part becomes short range with increasing n. The critical value n_c at which the liquid phase ceases to exist is ~ 11. This value could be ~ 12 if we take into account the possible defect of the GMWDA that the freezing line predicted by this theory falls at somewhat lower densities, yielding a higher triple point, than the true results. These values of n_c are compared with the MC result [11], $n_c \sim 10$, for the m–n–spline potential system. For C_{60} we have found that if one uses a 'truncated' potential the predicted liquid–vapour coexistence region is suppressed by ~ 100 K and becomes metastable since the sublimation line now passes about 50 K above the critical point. This result is qualitatively consistent with the corresponding MC simulations of Hagen *et al* [4], and provides a partial explanation for the discrepancy between the MC and MD simulations. The GMWDA predicts that C_{60} has a liquid phase in a very narrow range of temperatures (< 20 K) if the full Girifalco potential is assumed. If again we take into account the possible defect of the GMWDA mentioned above, the liquid phase of C_{60} could exist over a wider range of temperatures, which supports the result of MD simulations of Cheng *et al* [5].

Acknowledgments

This work has been financially supported by a grant-in-aid for scientific research on priority areas under No 07236105. Part of this work was carried out under the Visiting Researchers Programme of the Institute for Materials Research (IMR), Tohoku University. We would like to thank the Computer Centre at Iwate University and the HITACS-3800/380 supercomputing system at IMR for providing us with computing facilities.

References

[1] Gast A P, Hall C K and Bussel W B 1983 *J. Colloid Interface Sci.* **96** 251
[2] Ashcroft N W 1991 *Europhys. Lett.* **16** 355
Ashcroft N W 1993 *Nature* **365** 387
[3] Girifalco L A 1992 *J. Phys. Chem.* **96** 858
[4] Hagen M H J, Meijer E J, Mooij G C A M, Frenkel D and Lekkerkerker H N W 1993 *Nature* **365** 425
[5] Cheng A, Klein M L and Caccamo C 1993 *Phys. Rev. Lett.* **71** 1200
[6] Mederos L and Navascués G 1994 *Phys. Rev.* B **50** 1301
[7] Caccamo C 1995 *Phys. Rev.* B **51** 3387
[8] Hasegawa M and Ohno K 1996 *Phys. Rev.* E **54** 3928
[9] Smit B 1992 *J. Chem. Phys.* **96** 8639
[10] Hagen M H and Frenkel D 1994 *J. Chem. Phys.* **101** 4093
[11] Hafskjold B 1995 *NAIR Workshop 95 on Cluster Science (National Institute for Advanced Interdisciplinary Research, Tsukuba, Japan)*
[12] Cuadros F, Okrasinski W and Sanfeld A 1996 *J. Chem. Phys.* **104** 5594
[13] Mederos L and Navascués G 1994 *J. Chem. Phys.* **101** 9841

[14] Tejero C F, Daunoun A, Lekkerkerker H N W and Baus M 1994 *Phys. Rev. Lett.* **73** 752
[15] Lomba E and Almarza N G 1994 *J. Chem. Phys.* **100** 8367
[16] Coussaert T and Baus M 1995 *Phys. Rev.* E **52** 862
[17] Rosenbaum D, Zamora P C and Zukoski C F 1996 *Phys. Rev. Lett.* **76** 150
[18] Bolhuis P and Frenkel D 1994 *Phys. Rev. Lett.* **72** 2211
[19] Bolhuis P, Hagen M H J and Frenkel D 1994 *Phys. Rev.* E **50** 4880
[20] Likos C N, Németh Zs T and Löwen H 1994 *J. Phys.: Condens. Matter* **6** 10 965
Likos C N, Németh Zs T and Löwen H 1995 *J. Phys.: Condens. Matter* **7** 8215
[21] Rascón C, Navascués G and Mederos L 1995 *J. Phys.: Condens. Matter* **7** 8211
Rascón C, Navascués G and Mederos L 1995 *Phys. Rev.* B **51** 14 899
Rascón C, Navascués G and Mederos L 1995 *J. Chem. Phys.* **103** 9795
[22] Németh Zs T and Likos C N 1995 *J. Phys.: Condens. Matter* **7** L537
[23] Likos C N and Senatore G 1995 *J. Phys.: Condens. Matter* **7** 6797
[24] Denton A R and Ashcroft N W 1989 *Phys. Rev.* A **39** 4701
[25] Hasegawa M 1993 *J. Phys. Soc. Japan* **62** 4316
Hasegawa M 1994 *J. Phys. Soc. Japan* **63** 2215
[26] Hansen J-P and McDonald I R 1986 *Theory of Simple Liquids* 2nd edn (London: Academic)
[27] Curtin W A and Ashcroft N W 1986 *Phys. Rev. Lett.* **26** 2775
[28] Lutsko J F and Baus M 1991 *J. Phys.: Condens. Matter* **3** 6547
[29] Mederos L, Navascués G, Tarazona P and Chacón E 1993 *Phys. Rev.* E **47** 4284
[30] Rascón C, Mederos L and Navascués G 1996 *Phys. Rev. Lett.* **77** 2249
[31] Curtin W A and Ashcroft N W 1985 *Phys. Rev.* A **32** 2909
[32] Lutsko J F and Baus M 1990 *Phys. Rev.* A **41** 5547
[33] Laird B B and Kroll D M 1990 *Phys. Rev.* A **42** 4810
[34] Hafskjold B and Ratkje S K 1995 *J. Stat. Phys.* **78** 463
[35] Weeks J D, Chandler D and Andersen H C 1971 *J. Chem. Phys.* **54** 5237
[36] Hasegawa M 1995 *J. Phys. Soc. Japan* **64** 4242
Hasegawa M 1995 *J. Phys. Soc. Japan* **64** 4248
[37] Rosenfeld Y and Ashcroft N W 1979 *Phys. Rev.* A **20** 1208
[38] Verlet L and Weis J J 1972 *Phys. Rev.* A **5** 939
[39] Henderson D and Grundke E W 1975 *J. Chem. Phys.* **63** 601
[40] Hansen J-P and Verlet L 1969 *Phys. Rev.* **184** 151
[41] Panagiotopoulos A Z 1987 *Mol. Phys.* **61** 813